ICAS 2021 SHANGHAI
International Council of the Aeronautical Sciences
32nd Congress of the International Council of the Aeronautical Sciences
September 6-10, 2021 Pudong Shangri-La, Shanghai, China

DEFORMATION ANALYSIS OF C-SPAR COMPOSITE STRUCTURE DURING THE PREFORMING PROCESSING

Chen Fei[1], Chen Ping[1], Zhao Yueqing[1]

[1] Composite Center, Shanghai Aircraft Manufacturing Corporation Ltd., Shanghai 200346, China

Abstract

The C-spar structure was manufactured by the double diaphragm forming（DDF）process, and the in-plane buckling direction of the fiber was analyzed by the stripping method to obtain the forcing direction of the fiber during the preforming process. Combined with the macroscopic force analysis and the simulation result of the preforming process, the stress and deformation of the laminate in the process can be predicted. Thus, we can avoid and relieve the emerging of the wrinkles and buckling to get a product with high quality.

Keywords: hot diaphragm forming, C-shaped, defects, thermosetting composite

1. Introduction

In recent years, composite materials have been widely used in aircraft structures due to their advantages such as lightweight, high strength, high design, fatigue resistance, corrosion resistance and easy integration. In fact, the use of composite materials has become an important indicator to measure the advancement of aircraft. The amount of composite materials used has rapidly expanded from secondary load-bearing structures such as tail to main load-bearing structures such as wing and fuselage. The proportion of composite materials in Boeing B757 and B767 is only 4%, to 11% and 14% of Boeing B777 and Airbus A340, and 25% of Airbus A380. Now, the proportions of composite materials used in Boeing B787 and Airbus A350, which represent the highest level of civil aircraft manufacturing technology in the world, has reached 50% and 52%, respectively[1]. At present, the CR929 wide-body airliner jointly developed by China and Russia is also expected to use more than 50% composite materials, with almost the entire surface of the aircraft made of composite materials[2].

The composite structure is mainly used in the fuselage, wing and tail of the aircraft, among which the wing and tail are box structure, composed of upper and lower panels and wing spar. In addition to the normal flight load of the aircraft, the box section of the wing also bears the highly concentrated load from the engine, flaps, ailerons and spoilers. Among them, the role of the wing spar determines that it has the characteristics of bearing large force, large thickness and high precision. The commonly used wing spar is C-shaped[3].

Traditional hand lay-up process is often adopted to manufacture wing spar, the prepreg is laid on the forming die manually, and then the prepreg is formed manually. The advantages of this method are layer by layer forming, high flexibility and less restriction on the shape of parts. With increasing use of wing spar, this labor-intensive, time-consuming and bad quality stabilization process is being challenged[3]. Automation has become the main development direction of civil aircraft composite structure manufacturing. With the continuous progress of technology, foreign countries have carried out research on hot diaphragm preforming technology, which has been verified in European alcas program, and promoted its maturity. In A400M project, the combination of automatic tape laying and hot diaphragm forming technology has successfully prepared composite wing front and rear spars with a total length of more than 10 m. At present, there is still a big gap between the domestic hot diaphragm forming technology and the international leading level, especially in the wing spars and other large thickness structures. Gu et al.[4-6] prepared C-typed carbon fiber composites by a self-

made hot diaphragm molding device. The effects of molding temperature, molding rate and structure size on molding quality and interlayer friction were investigated. Wang et al. [7] prepared carbon fiber composite spar/rib parts by hot diaphragm forming process, and studied the influence of molding pressure, temperature and time on molding quality by characterizing the cured parts. Wang et al. [8,9] used hot diaphragm forming process to form C-shaped structure of thermosetting carbon fiber composites, and the influence of oven and autoclave curing methods on the forming quality of structural parts were compared. At the same time, the hot diaphragm forming process of thermosetting composite was numerically simulated, and the temperature, curing degree distribution, interlayer slip and curing deformation during the forming process were studied. At present, the domestic research on hot diaphragm forming process is limited to the influence of forming process parameters on the forming quality, and there is a lack of research on the causes of pre-forming defects.

In this work, through the analysis of the buckling direction in the process of defects and the stress direction in the process of preforming, the mechanism of defects is analyzed. Moreover, the experiment results are compared with the simulation results, the main reasons for the defects of hot diaphragm preforming are summarized, which provides guidance for the future development of hot diaphragm forming.

2. Experiment

2.1 Materials

The material used is unidirectional carbon fiber/epoxy resin prepreg CYCOM X850® (Cytec Co.) with 35 % resin weight content. The nominal cured thickness per ply of the prepreg is 0.19 mm. The external service life of the prepreg is 30 days, and the prepreg is stored in the refrigerator before the test. Process accessories are provided by Airtech company of the United States.

2.2 Hot diaphragm forming process

In diaphragm forming process, a laminated prepreg is placed between elastic diaphragms and a vacuum is drawn so that the deformation is achieved by the application of vacuum. There are two diaphragm forming options; using either a single diaphragm (Single Diaphragm Forming, SDF) or two diaphragms (Double Diaphragm Forming, DDF). The SDF is simple, while the DDF has better control over the preform of the laminated prepreg, which can form the parts with thicker thickness and more complex structure [9]. In this work, double diaphragm forming was adopted, the process is shown schematically in Figure 1.

After the flat laminated prepreg is laid up by the automatic tape laying machine, it is transferred to the hot diaphragm preheating bed, fixed by the upper and lower diaphragms and other auxiliary materials, and then transferred to the preheated tooling. There are infrared lamps above the vacuum bed to heat the flat laminated prepreg. After heating to the preformed temperature, the vacuum operation is carried out between the tool and the lower diaphragm to complete the forming process. After the end of the forming, the part was left to cool down.

As shown in Figure 2, the spar is C-typed structure with variable section and thickness. There is thickness transition in the length direction of the spar, and the flange has subsidence.

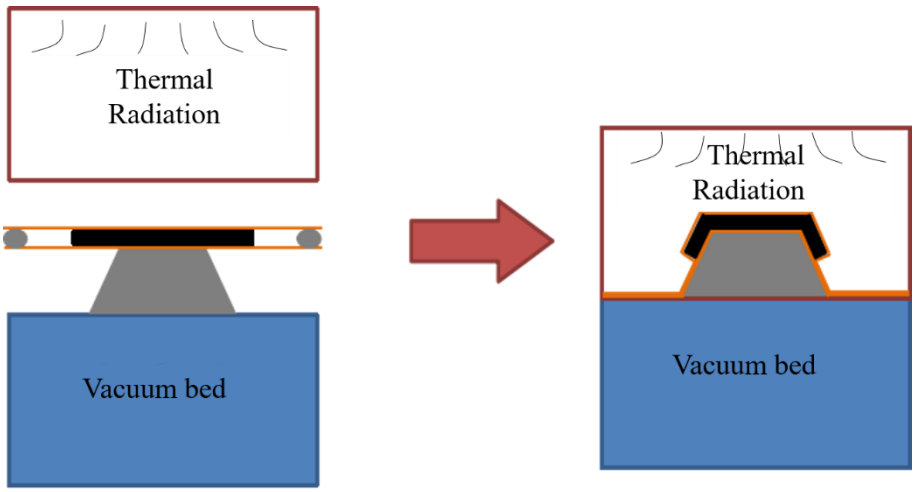

Figure 1 - Double diaphragm forming process.

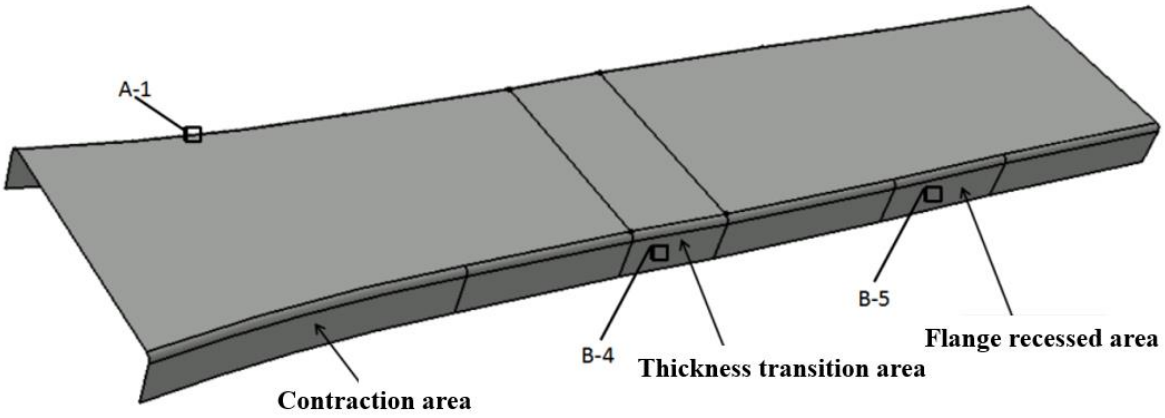

Figure 2 - The diagram of C-typed spar.

3. Results

3.1 Stress analysis of Fiber

The samples were taken in three typical characteristic areas, which were the contraction area (A-1), thickness transition area (B-4) and flange recessed area (B-5). The sample size is 3 cm * 3 cm. The specimen section is destroyed to facilitate peeling. The peeling is started from the die surface layer by layer, and the corresponding fiber direction and in-plane buckling direction are recorded. The specific peeling results are shown in Figure 3. In Figure 3, there was no in-plane buckling in the 0 ° layer and the 90 ° layer has a certain degree of buckling. Buckling was observed in the 135 ° layer both the two specimens at the fold and transition zone. But in the zone of flange recessed area, buckles can be observed in the 45 ° layer.

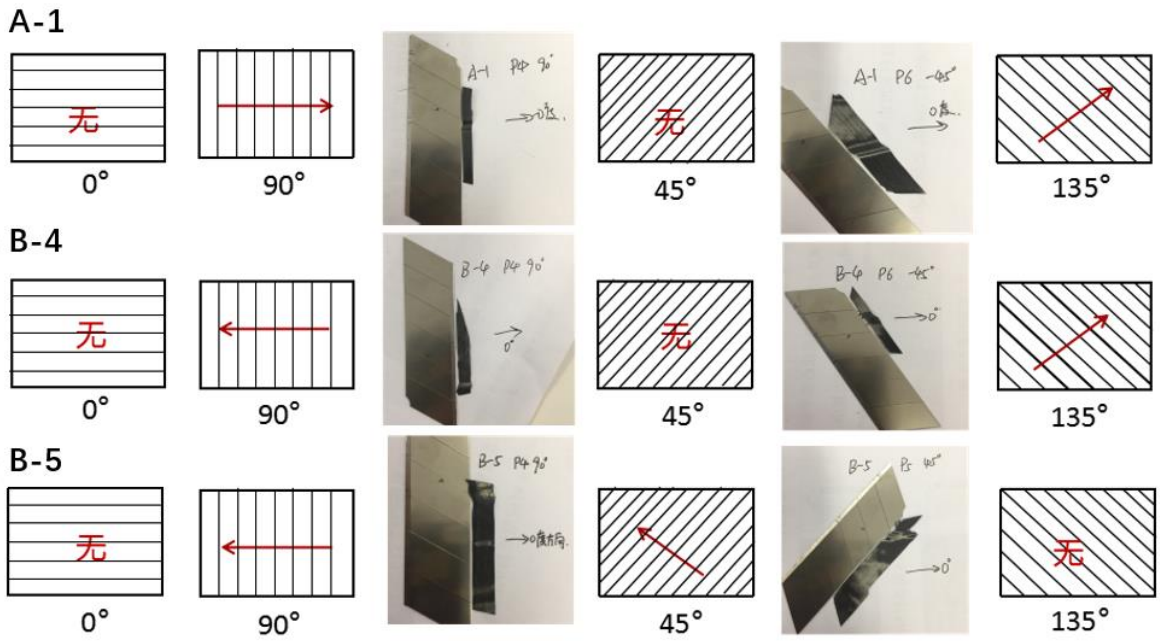

Figure 3 - Results of samples after peeling.

3.2 Macroscopic Stress Analysis of Laminates

The macro stress analysis in the preforming process is shown in Figure 4. A-1 is the sample at the necking position. During the forming process, the larger opening first contacted with the tooling, and other areas are shaped with the die under the pressure perpendicular to the laminate. As shown in Fig. 4 (a), F is the force which perpendiculars to the prepreg sheet but forms a certain angle with the die surface, so it is decomposed into the force F_1, which perpendiculars to the die surface, and the force F_2, which parallels to the die surface. The laminate is shaped by F_1, and F_2 causes the laminate to move towards the direction of smaller opening. Because the laminate is too rigid to move as a whole, the fiber in a specific direction (- 45 ° and 90 °) deformed in the process of sliding. Similarly, sample in B-4 was affected by F_1, resulting in buckling in - 45 ° and 90 ° layers, as shown in Fig. 4 (b). Sample in B-5 is affected by F_2, resulting in buckling in 45 ° and 90 ° layers, as shown in Figure 4 (c).

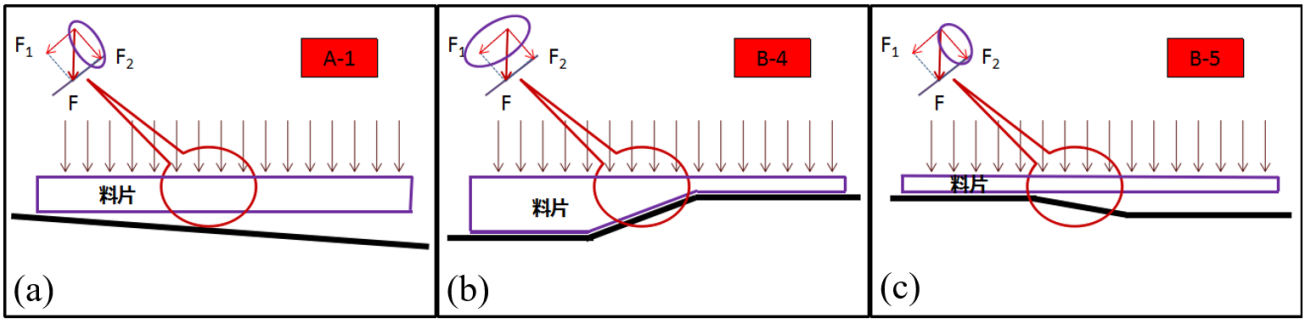

Figure 4 - Macro-stress analysis of specimen.

4. DDF process simulation

4.1 DDF process model

The typical characteristic thickness transition of the wing beam structure is taken as the characteristic to establish the simulation model, as shown in Figure 5. There is a width variation zone in the length direction of the model. In order to simulate the trend of stress distribution, the transition slope is designed as 1:5. A schematic figure of the FE-model is shown in Figure 6. The geometry in the FE-model consists of four parts: a base representing the fixed part of the DDF equipment, a forming tool, a prepreg sheet, and the diaphragms. For forming simulation, the tool and base were modelled as rigid bodies. Each ply was modeled by coupling solid element with membrane element. The rubber diaphragm is modelled with a Mooney–Rivlin material mode using S4 shell elements. Coulomb friction model was adopted for tool-diaphragm, diaphragm-prepreg and prepreg-prepreg contacts.

Average coefficients of friction used in the simulations were 0.15. Pressures of 0.1 MPa were applied to the upper surface of the bottom diaphragm and the lower surface of the top diaphragm to simulate the packaging of prepreg sheet. Then another pressure was applied on the upper surface of the top diaphragm, which increases slowly from 0 MPa to 0.1 MPa.

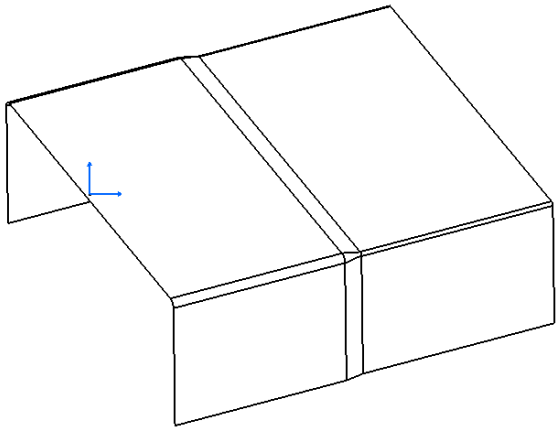

Figure 5 - Geometry used in the simulation.

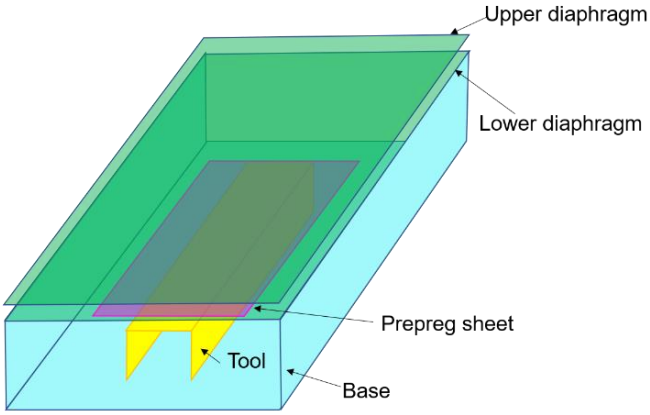

Figure 6 – The FE model of DDF process.

4.2 Simulation Results

4.2.1 Deformation of Diaphragm

Figure 7 and Figure 8 show the stress distribution of S11 and S22 of diaphragms, respectively. It can be seen from the Figures that when the fiber angle of prepreg is different, the stress distribution of diaphragm is quite different. For 0° and 90° fiber placement, the stress of the diaphragm is evenly distributed along the width direction. When the fiber angles of prepreg are 45° and - 45°, it can be found that the positions of the maximum stresses are symmetrical In addition, the positions where show the maximum stress are also the positions where prepreg wrinkle up.

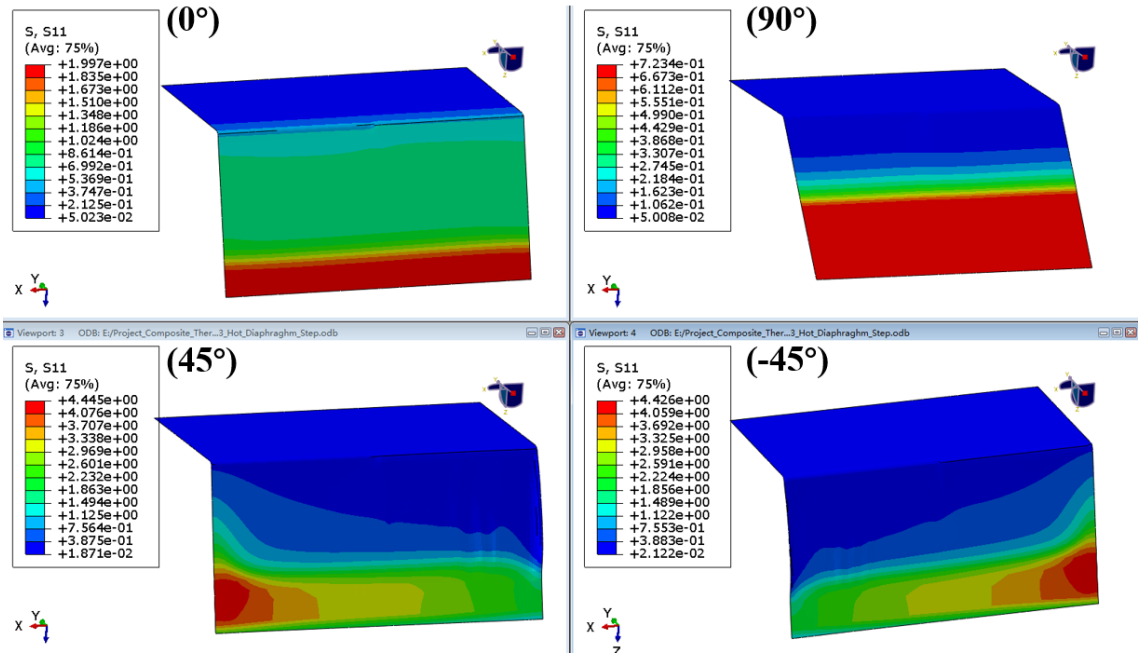

Figure 7 - S11 stress in the diaphragm of prepreg with different fiber angles.

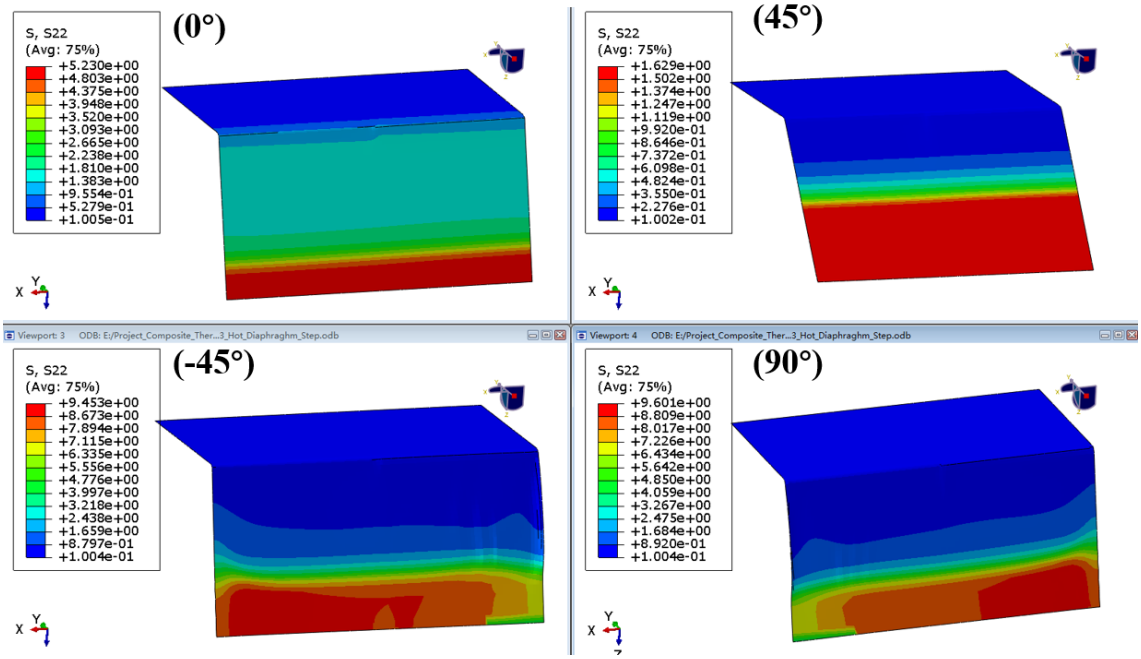

Figure 8 - S22 stress in the diaphragm of prepreg with different fiber angles.

4.2.2 Single-layer Prepreg

The hot diaphragm forming of single-layer prepreg with different angles is simulated and the results shown in Figure 9. For the 0°prepreg (see Figure 9(a)), there is no large wrinkle in the step area of the tool, but curl can be observed in the edge area of the prepreg which is along the transverse direction of the fiber. In Figure 9(b), there are two obvious wrinkles in the surface of 90° prepreg after deformation: one is in the step area of the tool, where the wrinkle extends from the step to the small end of the size change; the other is located at the web area of the large size area of the tool, and the wrinkles are parallel to the height direction of the tool. Obvious wrinkles can be observed in 45° ply and -45° ply. As shown in Figure 9(c) and 9(d), the prepreg at location 1 and 4 are easy to curl, and wrinkles at the web area and step area are pronounced. The position distribution of the wrinkles area of 45° ply and -45° ply are symmetrical along the length direction. It can be found from the deformation morphology shown in Figure 9 that although local uneven deformation is found in different angles, there are great differences in deformation mode and wrinkle degree.

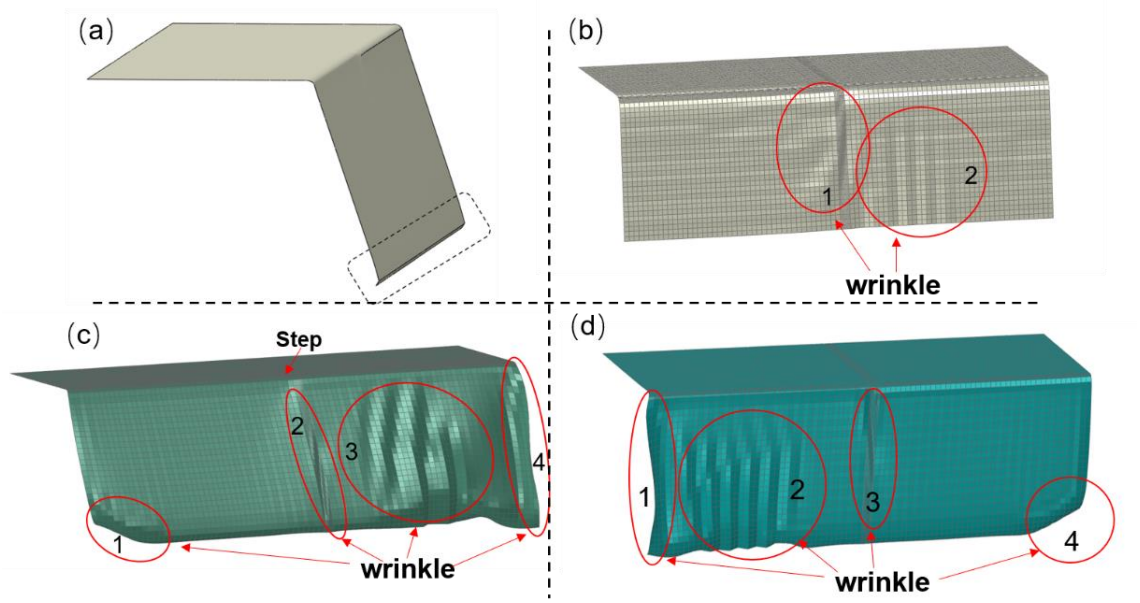

Figure 9 - Deformation of prepreg with different angles: (a) 0° ply; (b) 90° ply; (c) 45° ply; (d) -45° ply.

After comparing the stress distribution of the hot diaphragm, the stress distribution of the membrane element in the prepreg model was extracted. It can be seen from Figure 10, the stress concentration of 0° prepreg appears at the step. For the prepreg with 90° fiber angle, material accumulation occurs at the step, so the stress on the side with smaller width is lower. For the prepreg with fiber angles of 45 ° and - 45 °, there are large stress distribution in the R-angle regions, especially in the step position. In Figure 11, the S22 in 90° prepreg at location 2 is negative，therefore the material at this zone endure compress stress, which results in wrinkles, see Figure 9(b).

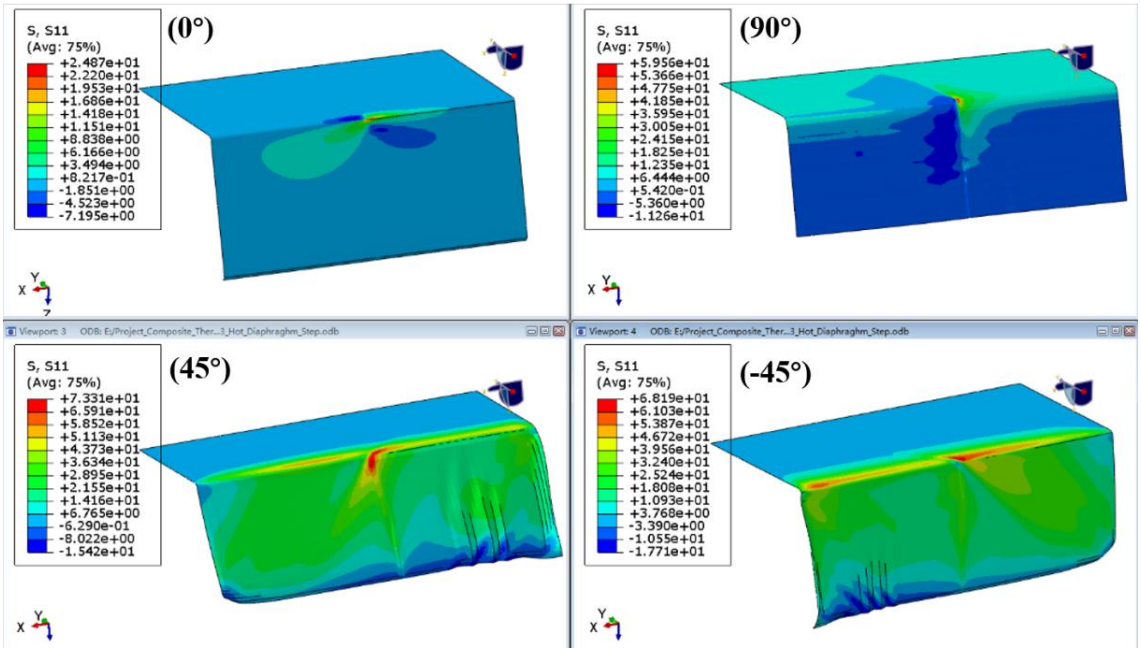

Figure 10 - S11 stress in the prepreg with different fiber angles.

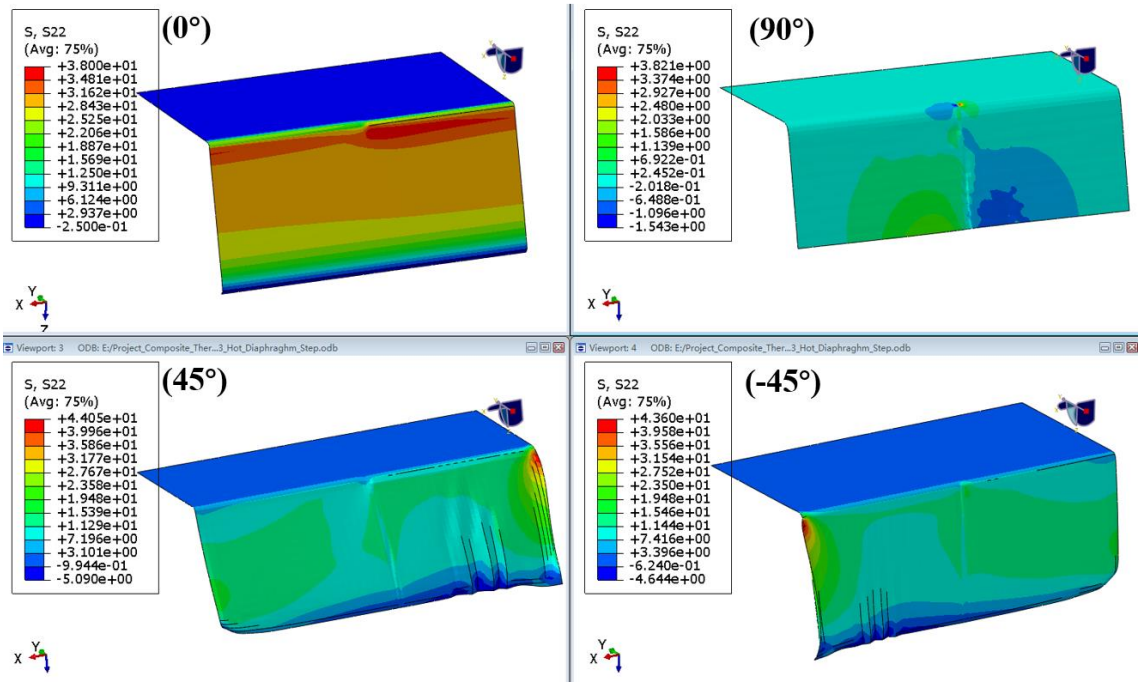

Figure 11 - S22 stress in the prepreg with different fiber angles.

Figure 12 shows the in-plane shear stress distribution of prepreg with different angles. It is obvious that the shear stress is low and the distribution area is small for the 0° prepreg and 90° prepreg. For 45° prepreg and - 45° prepreg, the shear stress is higher and the distribution area is wider. For unidirectional prepreg, the resistance to in-plane shear deformation is almost zero. For 45° prepreg and - 45° prepreg, the existence of large area of high shear stress leads to more wrinkles during deformation process.

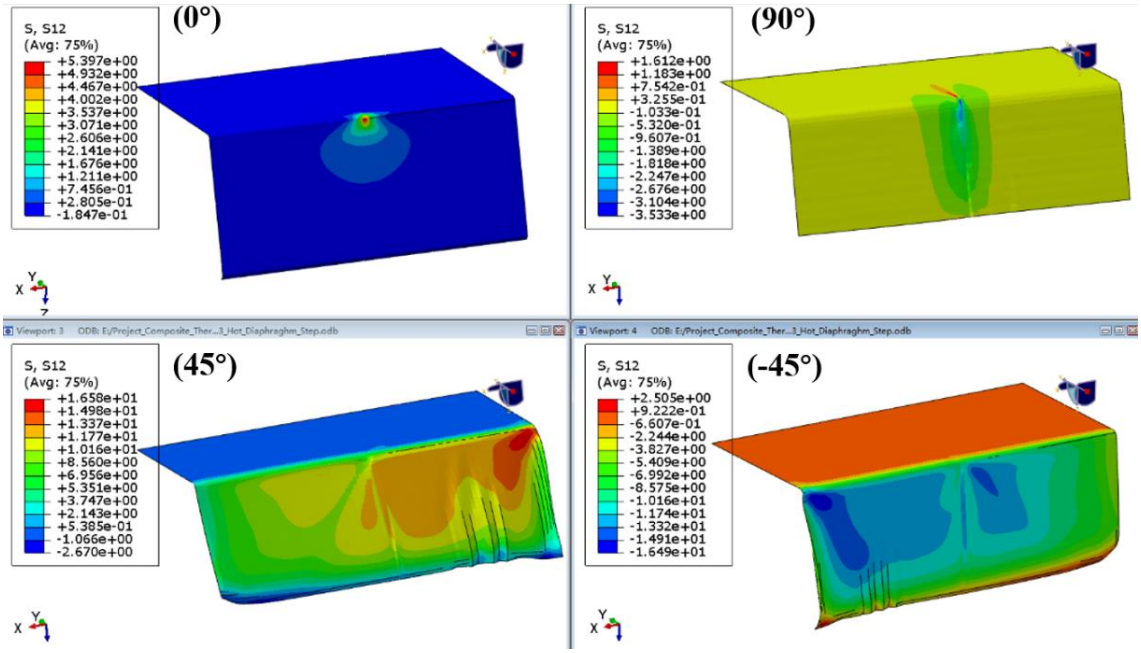

Figure 12 - S12 stress in the prepreg with different fiber angles.

4.2.3 Prepreg stack

Figure 13 shows the simulation results of the stacking sequence [0/45/90/-45]. Comparing with Figure 9 and Figure 13, it can be found that the deformation of single-layer prepreg is very different from that of prepreg stack. The prepreg stack has serious wrinkle at the step area. Two causes for wrinkles can be suggested, one is due to the excessive material and the other relating to the local compression in plies with fiber aligning with the direction of the compressive stress[10]. Figure 14 shows the stress distribution of different layers in the fiber direction. It can be seen that the wrinkle is consistent with the distribution of compressive stress. The wrinkle of the prepreg stack is caused by the compression

of the fiber. This is mainly due to the local uneven stress caused by the inconsistent shape of the stack and the tool.

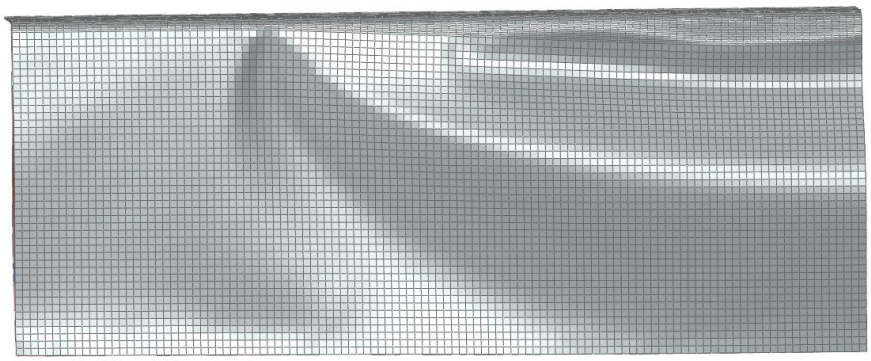

Figure 13 - Deformation of prepreg stack.

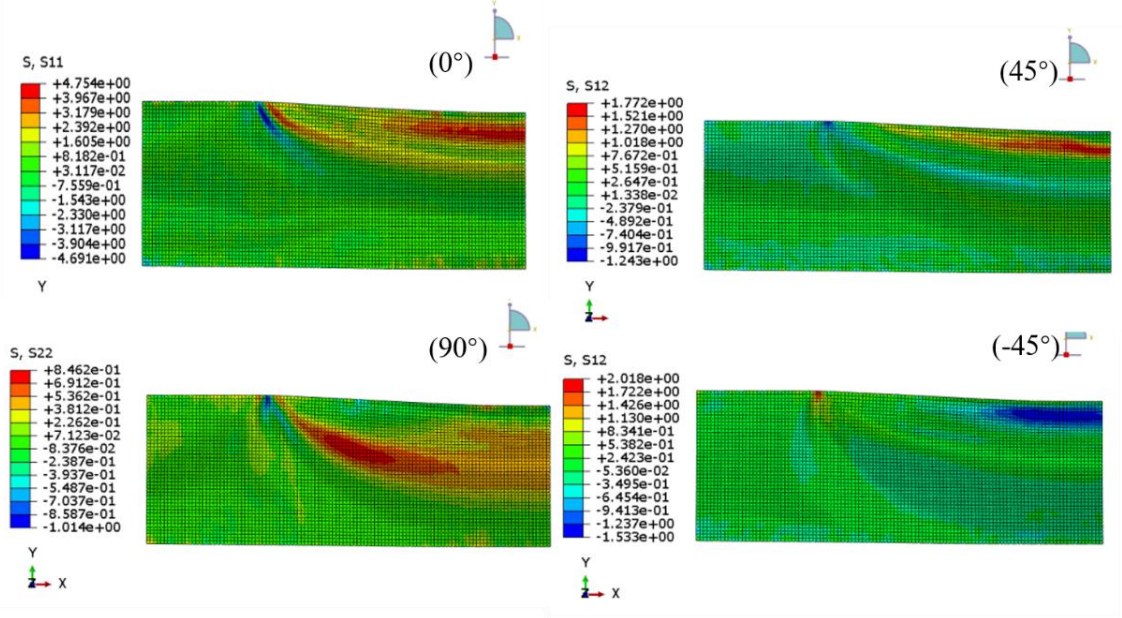

Figure 14 - Stress distribution of different layers.

5 Conclusions

In this paper, the C-spar structure was firstly manufactured by the DDF process, and the in-plane buckling direction of the fiber was analyzed by the stripping method to obtain the forcing direction of the fiber during the preforming process. Then the finite element model of single-layer prepreg is established, and the hot diaphragm forming of single-layer prepreg with different angles is simulated. For the single-layer prepreg, the wrinkle is controlled by the transverse stress and shear stress, and the wrinkle appears in the area with large transverse stress and shear stress. The in-plane properties of single-layer prepreg are seriously mismatched in fiber direction and transverse properties. During the deformation process of single-layer prepreg, the prepreg tends to deform towards the location with the weakest stiffness. For the prepreg stack, the wrinkle is no longer controlled by transverse stress and in-plane shear. As a whole, the defect of the laminate mainly occurs in the change area of geometry. In this area, due to the buckling of the fiber under pressure, the deformation can not be coordinated and local accumulation is formed.

References

[1]马立敏, 张嘉振, 岳广全等. 复合材料在新一代大型民用飞机中的应用[J].复合材料学报，32(2): 317-322,2015.
Ma Limin, Zhang Jiazhen, Yue Guangquan, et al. Application of composite in new generation of large civil aircraft[J]. Acta Materiae Compositeae Sinic Acta, Vol.32, No.2, pp 317-322,2015.
[2]马刚,张晓哲,唐文峰.大型复合材料加筋壁板自动化制造技术研究[J].航空制造技术,61(14):91-96,2018.
Ma Gang, Zhang Xiaozhe, Tang Wenfeng. Automated manufacturing technology of large stiffened panel[J]. Aeronautical Manufacturing Technology, Vol.61, No.14, pp 91-96,2018.

[3]杨博,王菲,陈永清.大尺寸复合材料翼梁的制造技术发展[J].航空制造技术, (22):74-77,2013.
Yang Bo, Wang Fei, Chen Yongqing. Manufacturing of Large Scale Composite Spar[J]. Aeronautical Manufacturing Technology, No.22, pp 74-77,2013.
[4]顾轶卓, 李敏, 李艳霞, 等. 飞行器结构用复合材料制造技术与工艺理论进展[J].航空学报, 36(8): 2773–2797, 2015.
Gu Yizhuo, LI Min, LI Yanxia, et al. Progress on manufacturing technology and process theory of aircraft composite structure[J]. Acta Aeronautica et Astronautica Sinica, Vol.36, No. 8, pp 2773–2797, 2015.
[5]姚双,李敏,顾轶卓等.碳纤维复合材料 C 形结构热隔膜成型工艺[J].北京航空航天大学学报, 39(01):95-99+104, 2013.
Yao Shuang, Li Min, Gu Yizhuo. Hot diaphragm forming of carbon fiber composite with C-shaped structure[J]. Journal of Beijing University of Aeronautics and Astronautics, Vol.39, No. 1, pp 95-99+104, 2013.
[6]边旭霞,顾轶卓,孙晶等.热隔膜工艺温度与成型速率对 C 形复合材料成型质量的影响[J].玻璃钢/复合材料, (05):45-50,2013.
Bian Xuxia, Gu Yizhuo, et al. Effects of temperature and molding rate hot diaphragm process in the forming quality of C-shaped composite[J]. Fiber Reinforced Plastics/Composites, No. 5, pp 45-50,2013.
[7]汪冬冬, 徐恒元, 龚志红, 李成龙. 碳纤维复合材料梁/肋零件热隔膜成型工艺研究[J].玻璃钢/复合材料,10:50-55,2016.
Wang Dongdong, Xu Hengyuan, Gong Zhihong,et al.Study On the hot diaphragm forming of carbon fiber composite with beam and rib parts[J]. Fiber Reinforced Plastics/Composites, Vol.10, pp 50-55, 2016.
[8]王永军,杨凯,陈森林等.热固性碳纤维编织复合材料C形结构隔膜成型工艺[J].玻璃钢/复合材料, (03):59-65,2015.
Wang Yongjun, Yang Kai, Chen Senlin, et.al. Hot-diaphragm forming of thermosetting carbon woven fabric composite with C-shaped structure[J]. Fiber Reinforced Plastics/Composites, No. 3, pp 59-65,2015.
[9]元振毅,王永军,杨凯等.热固性树脂基复合材料热隔膜成型过程数值仿真[J].复合材料学报,33(07):1339-1350,2016.
Yuan ZhenYi, Wang Yongjun, Yang Kai, et al. Numerical simulation for hot diaphragm forming process of thermosetting resin matrix composites[J]. Acta Materiae Compositeae Sinic Acta,Vol. 33, No.07, pp 1339-1350, 2016.
[10] Sjölander J, Hallander P , Sjölander M. Forming induced wrinkling of composite laminates: A numerical study on wrinkling mechanisms[J]. Composites Part A Applied Science & Manufacturing, Vol. 81, pp 41-51,2016.

Copyright Statement